Politecnico di Milano

Orbital Mechanics

Group 2153, A.Y. 2021/22

07/01/2022

Interplanetary Explorer Mission and Planetary Explorer Mission

Mads L.U. Larsen [10833041, 984967]
Federico Infantino [10808187, 996989]
Gloria Castronovo [10837697, 992130]
Riccardo Picozzi [10620335, 994918]

Contents

Contents ii

1 Interplanetary Explorer Mission 1

1.1 Introduction . . . 1
1.2 Preliminary Estimates . . . 1
1.3 Grid search . . . 3
1.4 Refined Grid search . . . 5
1.5 Advanced Algorithm . . . 8
1.6 Conclusion . . . 9

2 Planetary Explorer Mission 10

2.1 Introduction . . . 10
2.2 Nominal Orbit . . . 10
2.3 Ground track . . . 11
2.4 Repeating Ground track . . . 12
2.5 Perturbations . . . 13
2.6 Gauss Planetary Equations . . . 14
2.7 Filtering . . . 17
2.8 Comparison with real data . . . 17

Bibliography 19

Interplanetary Explorer Mission 1

1.1 Introduction

The PoliMi Space Agency is carrying out a feasibility study for a potential Interplanetary Explorer Mission visiting three planets in the Solar System. The planets involved in the mission can be seen on table 1.1, along with the departure and arrival windows.

Departure Planet	Flyby Planet	Arrival Planet
Jupiter	Mars	Venus

Earliest Departure	Latest Arrival
2026/04/01	2066/04/01

Table 1.1: Assigment data

The purpose of this chapter is to describe the preliminary mission analysis, carried out using the *Method of Patched Conics*, to evaluate the required Δv for mission success. The mission consists of two interplanetary transfer and a powered gravity assist to connect the two arcs. The analysis aim is to evaluate the mission window and find a lunch window with the overall lowest cost in terms of propellant powered manoeuvres, complying with departure and arrival time given and with the constraints on the flyby manoeuvre.

1.2 Preliminary Estimates

The time window given for the entire mission is 40 years, therefore looking for the best dates to minimize the mission cost is numerically expensive. It is necessary to perform a preliminary analysis to see if it is possible to shrink the time window down to a manageable size. This allows for a lower time difference between each time element but without deleting a part of the window in which an optimal solution could be found.

The first method to understand the ideal time window of the mission is to evaluate the Synodic period of the planets. This is relevant because it helps to choose the size of our search window showing how often the planets would be in an favourable position to perform a transfer.

The Synodic periods of Mars with respect to Jupiter and of Venus with respect to Mars are the following:

$$T_{syn_{JM}} = 2.2356\,\text{years} \tag{1.1}$$
$$T_{syn_{MV}} = 333.9\,\text{days} \tag{1.2}$$

Since Jupiter-Mars Synodic period is more than double the one of Mars-Venus, the transfer between the first two planets affects the cost and duration of the mission, if is performed in a non optimal way. In order to approximate the length of the whole mission, the TOF of a Hohmann transfer for both interplanetary legs is computed, giving a total length of 3.673 years.

Another tool used to understand how often the minimum Δv solution for the interplanetary transfers are repeated is the Pork-chop plot. The Pork-chop plots in Figure 1.1 to 1.2 on pages 2–3 are showing the necessary Δv required for the transfer from Jupiter to Mars, and from Mars to Venus. In particular, the Δv minimum contour lines for each interplanetary transfer and their repetitions are displayed.

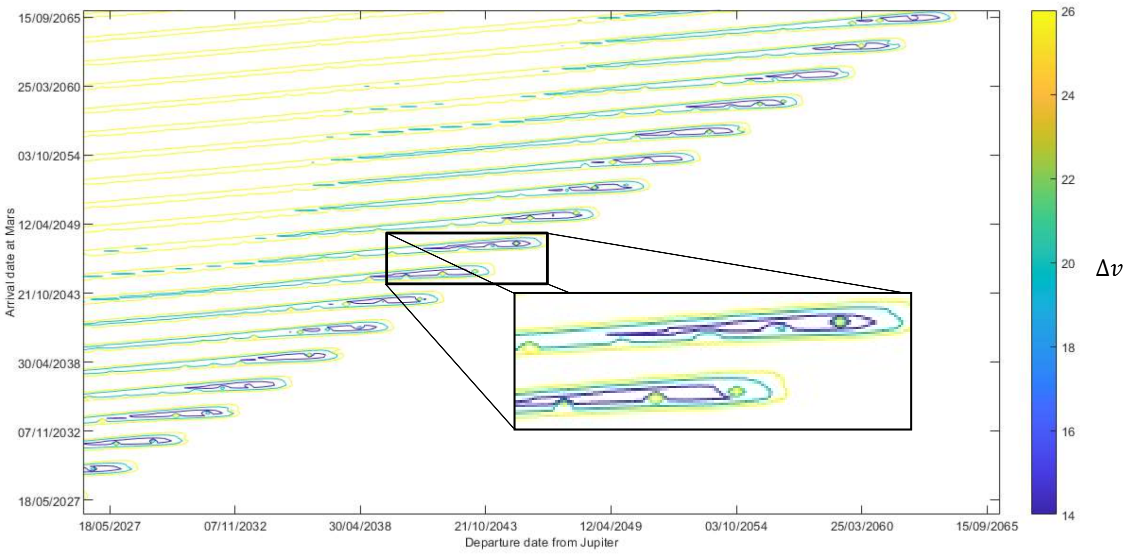

Figure 1.1: Pork chop plot of the transfer from Jupiter to Mars

From the Pork-chop plots it is evident that the optimal Δv transfers occur with a fixed repetition in time, in particular the transfer from Jupiter to Mars requires more time than the one from Mars to Venus and the dates associated to the minimum cost transfer are less frequent.

The Pork-chop plots are a useful tool, but they show sub-optimal results as it is only associated to a single part of the whole mission. The optimal solution for departure and arrival dates for the first interplanetary transfer could be non ideal for the second leg or for the flyby manoeuvre.

In the end, after having evaluated different tools for a preliminary analysis of the time window choice, it was decided to evaluate the whole time window of 40 years dividing it in 8 slots of 5 years each. It was chosen to divide it in 5 years because the total time of flight computed as the sum of the sub-optimal interplanetary transfers was of 3.5 years,

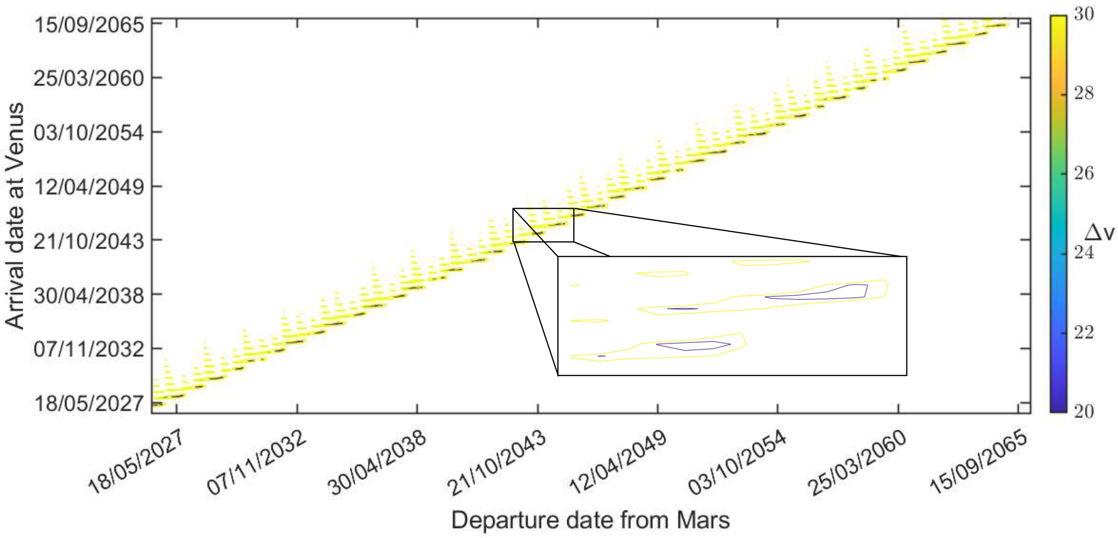

Figure 1.2: Pork chop plot of the transfer from Mars to Venus

but it was decided to give to this value a certain margin of uncertainty to be sure of not imposing any type of undesired constraint. In the following section, the *Grid Search Method* is going to be explained, and will be showing the results obtained for each of the eight slots. The minimum solution found will then be used for a refined research.

1.3 Grid search

The first approach used to compute the minimum cost for the whole mission Δv_{tot} is to perform a grid search through a *Triple Nested For loop* algorithm.

Algorithm 1 Triple Nested For loop

for Each Departure date from Jupiter (index i) **do**
  for Each Flyby date on Mars (index j) **do**
    if Mars Flyby Time - Jupiter Departure Time > 0 **then**
      Compute the Δv for the First Transfer Arc (Jupiter to Mars)
      for Each Venus Arrival Date (k) **do**
        if Venus Arrival Time - Mars Flyby Time > 0 **then**
          Compute the Δv for the Second Transfer Arc (Mars to Venus)
          if Flyby constraints are respected **then**
            Compute the Δv deriving from the Flyby on Mars
            Store the Δv_{tot} in the (i, j, k) cell of the 3D matrix
          end if
        end if
      end for
    end if
  end for
end for

1.3.1 Algorithm Description

As it could be seen from the algorithm scheme, the grid search looks for the minimum Δv_{tot} evaluating all the possible combinations between the discretized times of departure, flyby and arrival. Being an iterative algorithm with three nested loops it was necessary to choose time vectors with a limited amount of elements. In order to reduce the computational effort it was decided to use 100 elements vectors, therefore a total number of possible combinations equal to 100^3 is computed. An higher number of elements increases the accuracy of the search but at the same time the computational time required to do it became too large, making the algorithm inefficient.

The algorithm has multiple *if conditions* to check that only feasible transfers are computed. In particular there are two conditions regulating the time vectors in order to always have: time of arrival bigger than time of departure, and to have the radius of periapsis of the hyperbola bigger than the minimum one, computed as the radius of Mars plus the height of its atmosphere. Further details about the flyby manoeuvre and the importance of applying the constraint are explained in Section 1.4.1.

For each part of the mission the corresponding Δv is evaluated. In the second loop, through the solution of the Lambert problem, the required Δv_1 is computed, given by the sum of the Δv required to inject the S/C in the interplanetary arc and the Δv required to exit from it. In the third loop, the required Δv_2 of the second interplanetary transfer is computed. With the injection velocity on Mars coming from the first Lambert problem and the outgoing velocity from Mars coming form the second Lambert problem, the third loop is computed Δv_{GA} as the cost required to perform the flyby manoeuvre having those velocities.

After having explained how Δv_{tot} is computed, it is necessary to clarify how the minimum could be found. The following algorithm scheme shows the logic implemented to compute the minimum cost of the mission.

Algorithm 2 Finding the minimum Δv and its indeces

Initialize $\Delta v_{guess} = 10^8$
if $\Delta v(i,j,k) < \Delta v_{guess}$ **then**
  $\Delta v_{guess} = \Delta v(i,j,k)$
  IG $= i$
  JG $= j$
  KG $= k$
end if

At each time step of departure, flyby and arrival times the Δv_{tot} in the position (i,j,k) of the 3D matrix is compared with a value Δv_{guess} initialized to 10^8 to be sure that in the first iteration the if condition is respected. If the statement is verified the guess value becomes the Δv_{tot} in the (i,j,k) position. These indices are saved to compute the optimal dates (and other parameters) in which we have the minimum cost.

1.3.2 Grid Search Results

According to the preliminary estimates, it was chosen to compute the minimum Δv_{tot} with a time window of 5 years dividing the 40 years window assigned, between 1st April 2026 and 1st April 2066, in 8 consecutive slots.

The search for the overall minimum cost of the mission has been performed with the same time window both for the departure, flyby and arrival time vectors. Having a 100 elements vectors the Δt time difference between each discretized elements are of 18.26 days. For each consecutive time window of 5 years, the algorithm has been run and the results in terms of cost and optimal dates have been compared.

The best solution is obtained in the slot from 1st April 2036 to 1st April 2041, and it is the one in the following table:

	Departure	Flyby	Arrival	Total Cost
Date	12-11-2037	28-6-2040	17-10-2040	
Δv	26.3981 $\frac{\text{km}}{\text{s}}$	4.4277 $\frac{\text{km}}{\text{s}}$	24.7301 $\frac{\text{km}}{\text{s}}$	55.5559 $\frac{\text{km}}{\text{s}}$

Table 1.2: Grid Search method results

Due to the high total cost found it was decided to run again the algorithm with time windows of 10 years, to check if the 5 years window was too short and it constrained the problem. However,in this case the best solution is obtained in the slot between 1st April 2036 and 1st April 2046 giving the same results for departure, flyby and arrival dates, and giving the same result in terms of Δv_{tot}. This confirms that the preliminary time estimation was correct and that the best solution is the one shown in the table 1.2.

1.4 Refined Grid search

The solution obtained in the previous section can be refined in different ways. Starting from the optimal dates it was decided to reduce the time window, in particular, the departure date from Jupiter found is the 12th November 2037, so the beginning of the time window has been set to 1st June 2037, still keeping a margin to avoid constraints. Moreover, it has been imposed as the last arrival date the 1st June 2041. The new time window of 4 years has been divided into 200 elements discretized vectors with a time difference between each element of 7.3 days.

The accuracy has more than doubled, but at the same time the computational effort required has increased of eight times. The results obtained are shown in the following table.

	Departure	Flyby	Arrival	Total Cost
Date	2-11-2037	28-6-2040	16-10-2040	
Δv	26.2965 $\frac{\text{km}}{\text{s}}$	4.3114 $\frac{\text{km}}{\text{s}}$	24.7938 $\frac{\text{km}}{\text{s}}$	55.4017 $\frac{\text{km}}{\text{s}}$

Table 1.3: First Refined Grid Search results

The dates and the Δv_{tot} are very similar compared to the one obtained with the Grid Search, so increasing even more the number of elements of the time vectors would have not increased the accuracy efficiently. Therefore too refine the solution, the accuracy of the matlab *fsolve function* has been increased from its standard value of 10^{-6} to 10^{-12}. The results obtained are shown in the following table.

	Departure	Flyby	Arrival	Total Cost
Date	30-6-2037	5-7-2040	16-10-2040	
Δv	24.2131 $\frac{\text{km}}{\text{s}}$	0.8578 $\frac{\text{km}}{\text{s}}$	27.3151 $\frac{\text{km}}{\text{s}}$	52.3859 $\frac{\text{km}}{\text{s}}$

Table 1.4: Second Refined Grid Search results

As it could be seen the Δv_{GA} is way lower than the one obtained previously, but the Δv_2 of the second interplanetary leg has increased. The overall cost Δv_{tot} of the mission is the lower obtained with the Algorithm and the most accurate.

The dates and cost computed in this last method are considered the optimal ones for the *Refined Grid Search*, so they are taken as the starting point for considerations on the manoeuvres, plots and computation of other parameters.

1.4.1 Power Gravity Assist

This section will present the relevant data and supporting figures for the powered gravity assist with Mars. The gravity assist is illustrated on figure 1.3, here the incoming and outgoing hyperbolas are visible along with the Δv line. The position of the perigee is:

$$\underline{r}_p = \begin{bmatrix} 555.7\,\text{km} \\ -3163.7\,\text{km} \\ 1669.3\,\text{km} \end{bmatrix} \tag{1.3}$$

This gives a perigee height of 230 km above the martian surface, which is 80 km above the minimum required height of 150 km. The minimum height was calculated using NASA (2021) model for approximating the pressure for the martian atmosphere. The maximum height for the atmosphere was calculated by approximating the vacuum of space to 0.000 001 kPa, this returns a height of 150 km.

The Gravity assist will occur on the 5^{th} of July 2040 at 14:57 o'clock, where the spacecraft will be at the perigee point. The total gravity assist can be seen from when the spacecraft enters and exists Mars' SOI. In order to compute the time spent inside Mars finite SOI, the SOI radii is calculated as follows:

$$r_{SOI_M} = R_M \left(\frac{m_M}{m_S}\right)^{\frac{2}{5}} = 623\,300\,\text{km} \tag{1.4}$$

To find the time of entry and exit, the two opposite hyperbola orbits was computed so it was possible to locate two $r_{\vec{s/c}}$ point pairs, with one inside and the other point outside the SOI. A linear model was used to interpolate between data points and calculate the time corresponding to when the spacecraft position would have a norm exactly equal to r_{SOI_M}. This gives a total time spent inside Mars' SOI equal to 20.24 h.

The table below present the relevant data from the gravity assist, and the following figure 1.3 will illustrate the gravity assist:

R_p	h_p	ΔV	Δv_p	δ	δ_{minus}	δ_{plus}	β_{minus}	β_{plus}
3620 km	230 km	1.4751 $\frac{km}{s^2}$	0.858 $\frac{km}{s^2}$	4.53°	4.31°	4.76°	87.85°	87.62°

Table 1.5: Gravity assist data

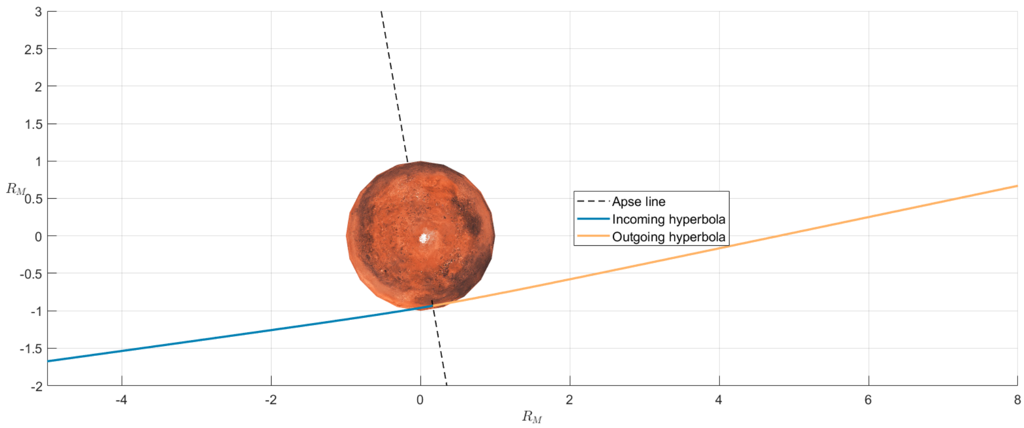

(a) Top view

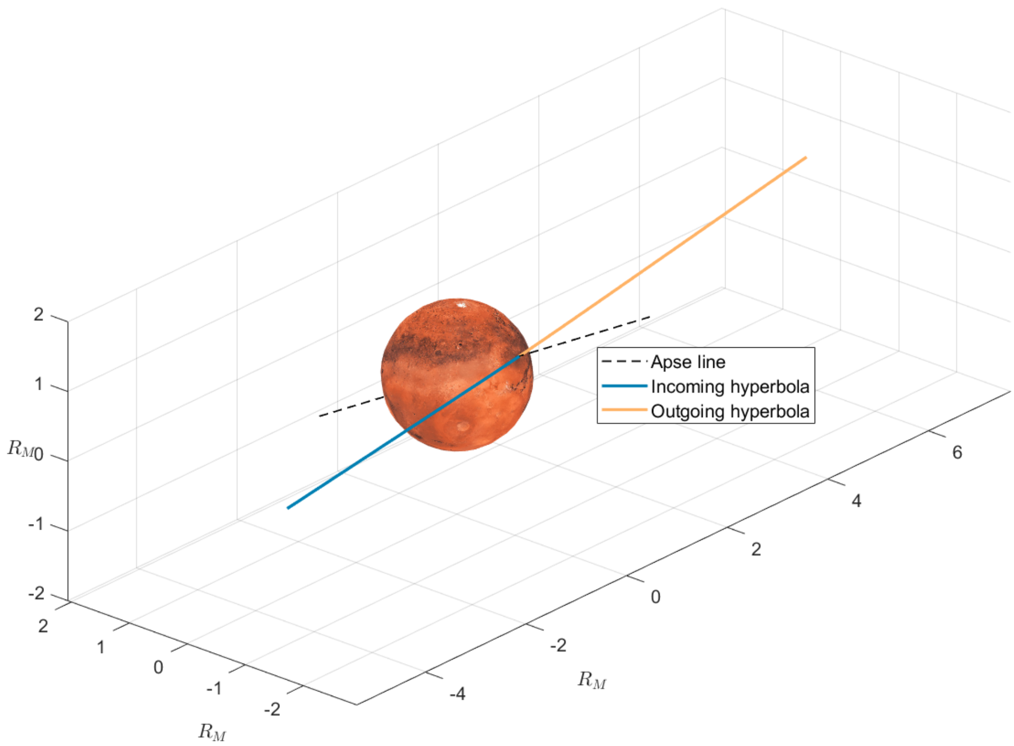

(b) Side view

Figure 1.3: Gravity assist around Mars

1.4.2 Heliocentric Transfer Arcs

Heliocentric interplanetary transfers have been computed solving two Lambert problems. The first interplanetary arc connects Jupiter and Mars and it is characterized by the following Keplerian elements.

a	e	i	Ω	ω	θ
4.5888×10^8 km	0.7434	0.0232 rad	1.7590 rad	3.2563 rad	2.9836 rad

Table 1.6: First interplanetary transfer Keplerian elements

The second interplanetary arc connects Mars and Venus and it is characterized by the following Keplerian elements.

a	e	i	Ω	ω	θ
3.5882×10^8 km	0.6966	0.0369 rad	0.7504 rad	4.4061 rad	4.3448 rad

Table 1.7: Second interplanetary transfer Keplerian elements

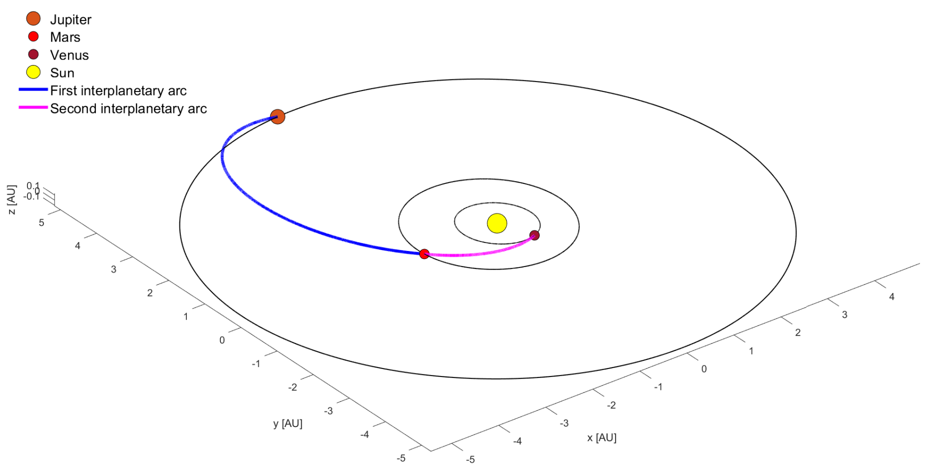

Figure 1.4: Interplanetary transfer

1.5 Advanced Algorithm

A further analysis of the mission has been performed with a constrained non linear multi-variable function solver. The matlab function used is *fmincon*, that looks for the minimum of a function imposing some constraints through inequalities and equalities. The function that is minimized has three inputs: the departure, fly-by and arrival dates. Instead, the output of the function, so what is going to be minimized, is the Δv_{tot}.

Fmincon searches for the minimum around an initial guess, that is put equal to the dates of departure, flyby and arrival obtained in the research grid search. The constraints are applied on the time vectors through the inequalities $A\,x \leq b$, where it's imposed that time of arrival to one planet has to be bigger than the time of departure from the previous one. Moreover, the search of the minimum is performed imposing a lower and upper boundary of dates, that were chosen to be of two months before and after the initial guess dates. It's imposed also a non linear constraint for the radius of periapsis of the flyby manoeuvre with a function that computes r_p still having as inputs the dates. The results obtained with this method are the following.

	Departure	Flyby	Arrival	Total Cost
Date	30-4-2037	8-7-2040	23-10-2040	
Δv	$23.3632\,\frac{\mathrm{km}}{\mathrm{s}}$	$4.584 \times 10^{-6}\,\frac{\mathrm{km}}{\mathrm{s}}$	$27.6248\,\frac{\mathrm{km}}{\mathrm{s}}$	$50.9880\,\frac{\mathrm{km}}{\mathrm{s}}$

Table 1.8: Fmincon Algorithm results

1.6 Conclusion

Using a simple grid search approach the minimum Δv for the entire mission is $52.39\,\frac{\mathrm{km}}{\mathrm{s}^2}$, with the following dates:

Departure: 30/06/2037 8:48
Flyby: 05/07/2040 14:57
Arrival: 16/10/2040 09:46

This result is obtained with high accuracy having a Δt between time elements of 7.3 days. Nonetheless, the refined grid search method could be improved even more increasing the number of elements of each time vector and at the same time imposing a condition on the time of flight, to compute only the transfer in a specific range of mission duration. This additional condition is needed to reduce the computational cost.

Using fmincon the minimum Δv was reduced by 2.67 % to $50.99\,\frac{\mathrm{km}}{\mathrm{s}^2}$, the dates changed as well to:

Departure: 30/04/2037 06:06
Flyby: 08/07/2040 12:24
Arrival: 23/10/2040 04:02

The difference in the two results depends on how the constraint on the radius of periapsis is imposed inside the two algorithms. The fmincon approach has a lower computational cost than the grid search, so it is much faster. On the contrary, fmincon is a less general method to compute the mission cost because it can only look for the minimum in a specific point of the time window.

Planetary Explorer Mission 2

2.1 Introduction

The following chapter will be focused on a Planetary Explorer mission, in order to perform Earth observation. Firstly, orbit analysis and ground track estimation are performed. This will give information about which area of the Earth is covered by the S/C trajectory and which will be characterized by the repeating ground track, obtained through the computation of a repeating semi-major axis. Moreover, it is necessary to understand the effects of orbit perturbations and to consider that different propagation methods are available and compare them.

2.2 Nominal Orbit

The nominal orbit of this mission is characterized by the following Keplerian elements shown in Table 2.1, with which it is possible to represent graphically the shape of the orbit in space, through its propagation.

a [km]	inc [deg]	e [-]	RAAN [deg]	ω [deg]	θ_0 [deg]
$2.6556 \cdot 10^4$	63.7406	0.6636	0	0	0

Table 2.1: Assigment 2 data

By integrating the equations of motion for the spacecraft around Earth, a state vector is obtained, describing the evolution of the position in time for one orbit.

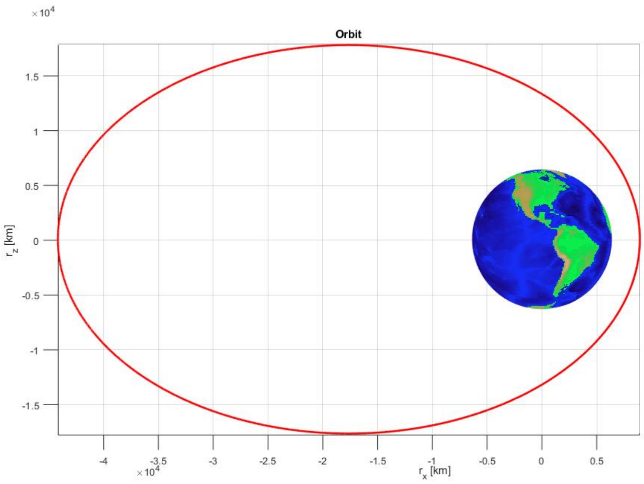

Figure 2.1: View 1

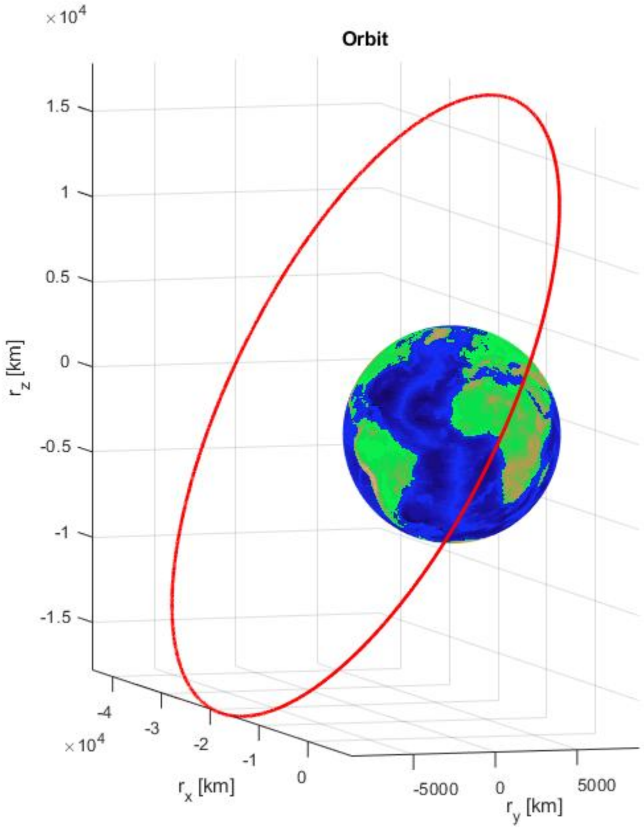

Figure 2.2: View 2

2.3 Ground track

As it is possible to propagate the orbit of the S/C around a planet, it is also possible to reproduce the ground track, which provides the instantaneous projection of the S/C orbit onto the planet surface. The representation of the nominal orbit ground track doesn't provide information about the behaviour of the S/C in case of perturbations.

The following figures will be related to the unperturbed two body problem, representing the ground track propagation over 1 orbit, 1 day and 10 days. Although not considering the perturbations, the path of the spacecraft is not repeating itself because it has a relative motion with respect to the Earth, so the ground track advances westward by an angle $\Delta\lambda$ equal to Earth's rotation during one orbital period T of the satellite.

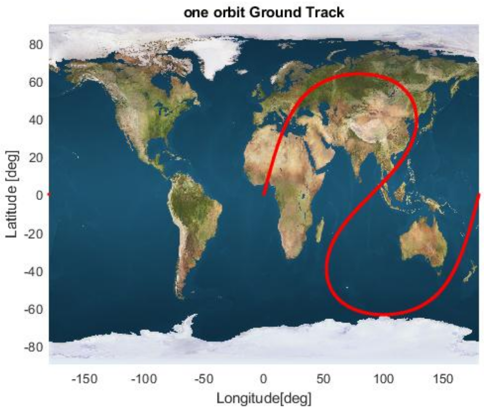

(a) One orbit unperturbed ground track

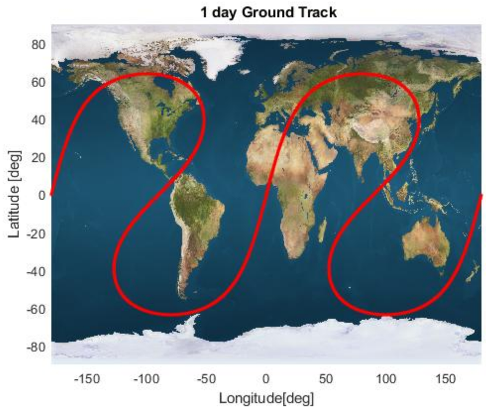

(b) 1 day ground track

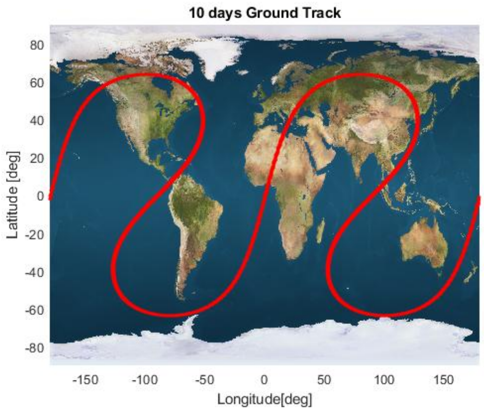

(c) 10 days ground track

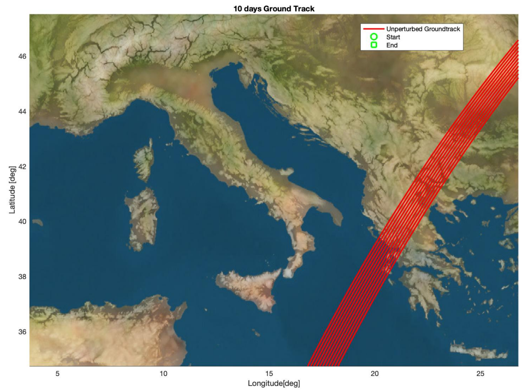

(d) 10 days ground track Zoom

Figure 2.3: Ground track

2.4 Repeating Ground track

To eliminate the shifting between two consecutive ground tracks, in order that the ground track can be able to repeat itself after k revolutions of the satellite and m rotations of the planet, it is possible to implement a function that provides the repeated semi-major axis. In the following figures the behaviour of the repeating ground track is shown.

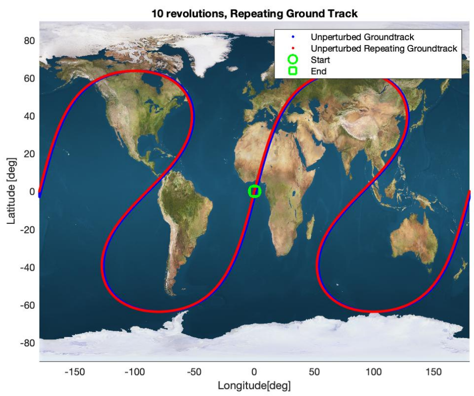

(a) Repeating Ground track 10 revolutions

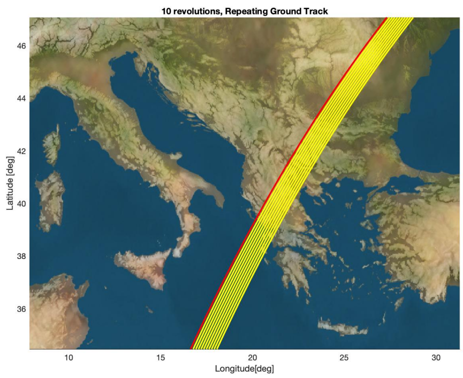

(b) Comparison between repeating (red) and nominal ground track (yellow)

Figure 2.4: Repeating ground track

2.5 Perturbations

The two most relevant perturbations considered, consist of two accelerations which have to be added to the equations of motion. Using these perturbations during the integration will yield the state vector, necessary for the orbit propagation, which in this case will be different from the nominal one.

Their expressions can be summarized as Curtis, 2004:

$$a_{J_2} = \frac{3}{2}\frac{J_2 \mu R_e^2}{r^4}\left[\frac{x}{r}\left(5\frac{z^2}{r^2}-1\right)\hat{\mathbf{i}} + \frac{y}{r}\left(5\frac{z^2}{r^2}-1\right)\hat{\mathbf{j}} + \frac{z}{r}\left(5\frac{z^2}{r^2}-3\right)\hat{\mathbf{k}}\right] \tag{2.1}$$

$$a_{moon} = \mu_{\mathrm{m}}\left(\frac{\mathbf{r}_{\mathrm{m/s}}}{{r_{\mathrm{m/s}}}^3} - \frac{\mathbf{r}_{\mathrm{m}}}{r_{\mathrm{m}}^3}\right) \tag{2.2}$$

The first perturbation is due to the oblateness of the Earth and it is known as J2 effect, or "Zonal Harmonic Potential at Second order term". The second perturbation represents the moon perturbation since it is a third body in a sufficient proximity of the satellite to influence him with his gravitational attraction. The perturbations affect the orbit and then the groundtrack, as showed below; using the semimajor axis for a repeating groundtrack does not make the groundtrack repeated, because including the perturbations the repeating semimajor axis can't be computed as before, since all the keplerian elements change over time and the previous relation is no longer valid.

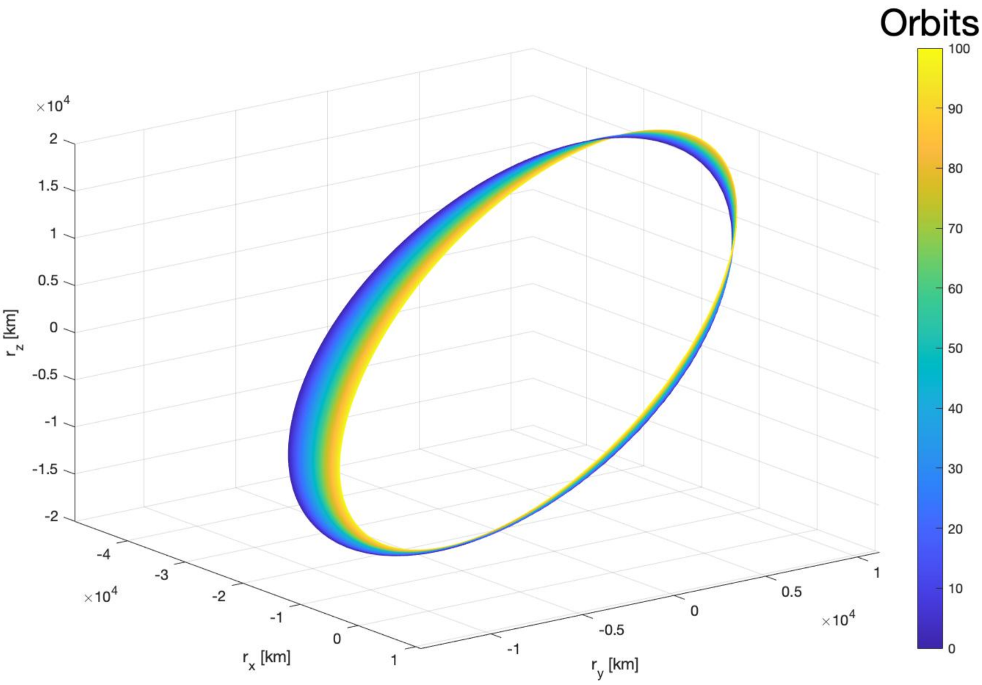

Figure 2.5: Perturbed orbit evolution

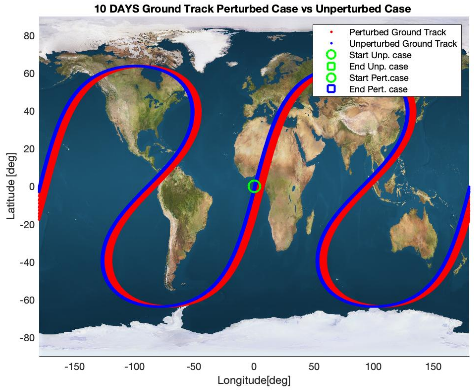

(a) 10 days groundtrack perturbed vs unperturbed case

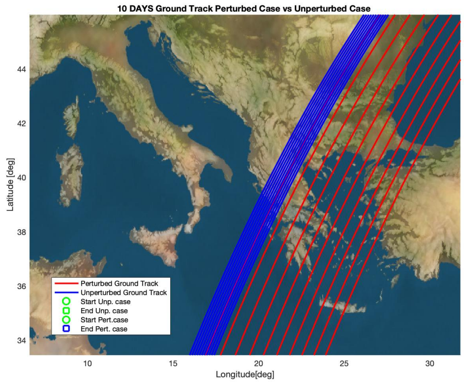

(b) Zoom

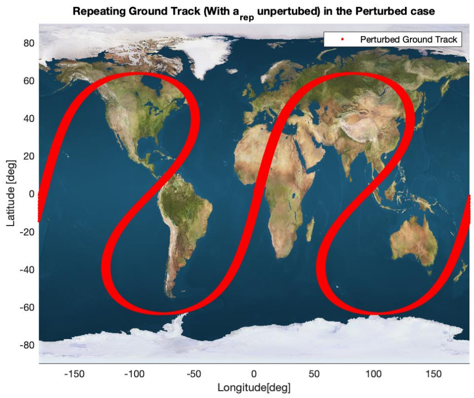

(c) Using repeating semimajor axis in the perturbed case

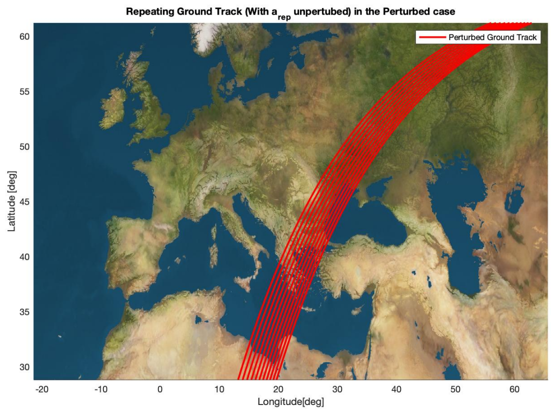

(d) zoom

Figure 2.6: Perturbed ground track

2.6 Gauss Planetary Equations

The evolution of Keplerian elements can be computed through a set of differential equations called Gauss Planetary Equations. These equations, as shown below, involve the perturbing acceleration given by the sum of the perturbing accelerations, in our case expressed in a tangential-normal-out of plane reference frame. Curtis, 2004

$$\frac{da}{dt} = \frac{2a^2\, v\, a_t}{\mu} \tag{2.3}$$

$$\frac{de}{dt} = \frac{1}{v}\left(2\left(e+\cos\left(\theta\right)\right)a_t - \frac{r}{a}\sin\left(\theta\right)a_n\right) \tag{2.4}$$

$$\frac{di}{dt} = \frac{r\cos\left(\theta+\omega\right)a_t}{h} \tag{2.5}$$

$$\frac{d\Omega}{dt} = \frac{r\sin\left(\theta+\omega\right)a_h}{h\sin\left(i\right)} \tag{2.6}$$

$$\frac{d\omega}{dt} = \frac{1}{e\,v}\left(2\sin\left(\theta\right)a_t + \left(2e+\frac{r}{a}\cos\left(\theta\right)\right)a_n\right) - \frac{r\sin\left(\theta+\omega\right)\cos\left(i\right)a_h}{h\sin\left(i\right)} \tag{2.7}$$

$$\frac{d\theta}{dt} = \frac{h}{r^2} - \frac{1}{e\,v}\left(2\sin\left(\theta\right)a_t + \left(2e+\frac{r}{a}\cos\left(\theta\right)\right)a_n\right) \tag{2.8}$$

Integrating numerically these equations, the orbit through Gauss equations over 100 periods is propagated. The evolutions of the Keplerian elements is then shown below, including a comparison with the propagation of the orbit in Cartesian coordinates obtained with the differential solver of the Perturbed Two Body problem dynamics. Analyzing the evolution of the elements it is possible to observe that every curve has different oscillations where different behaviours can be distinguished: secular variations, long-period and short-period variations. The shape of these evolutions are strictly connected to the perturbations considered. The results obtained with the two propagation methods are similar and the relative errors are in the range 10^{-3} to 10^{-4}. The propagation through Gauss Planetary Equations in this case results to be 14.98 % faster than the propagation in Cartesian coordinates using the two body problem differential solver.

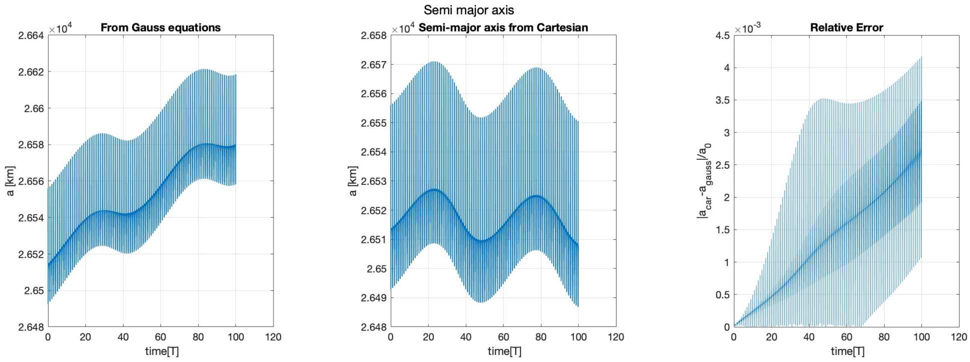

Figure 2.7: Semi-major axis evolution

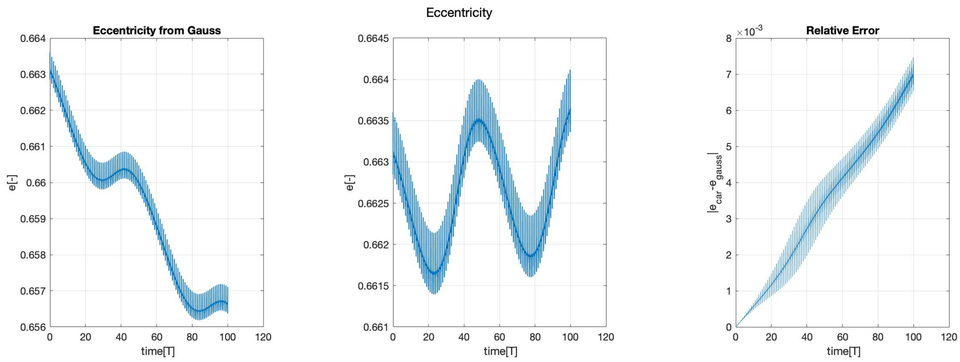

Figure 2.8: Eccentricity evolution

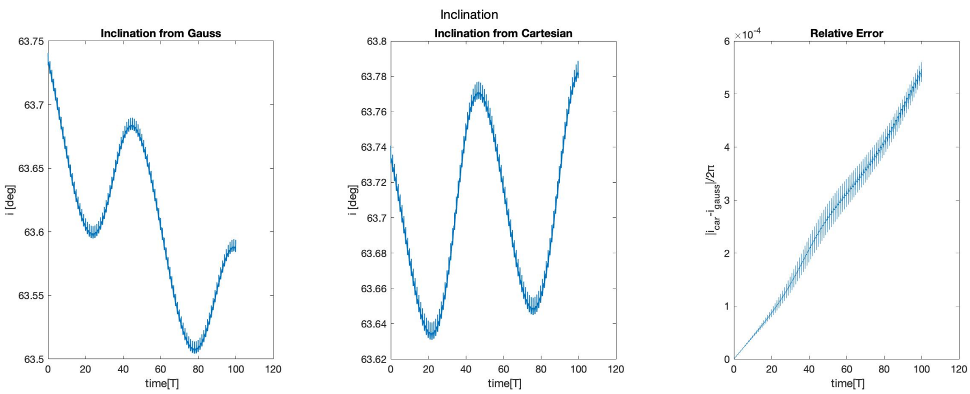

Figure 2.9: Inclination evolution

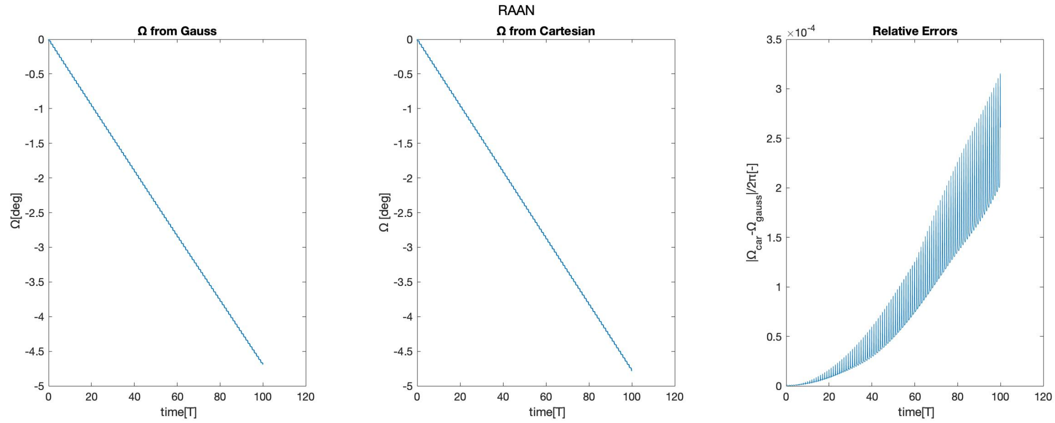

Figure 2.10: Ω evolution

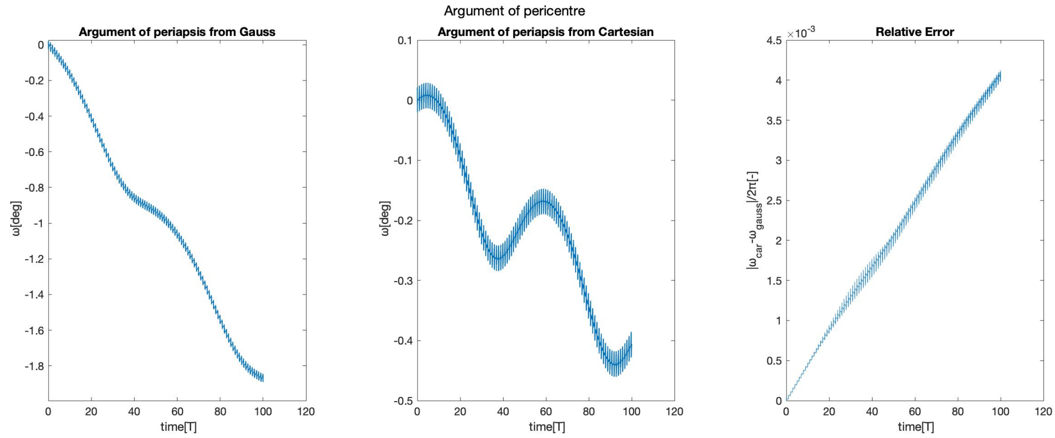

Figure 2.11: ω evolution

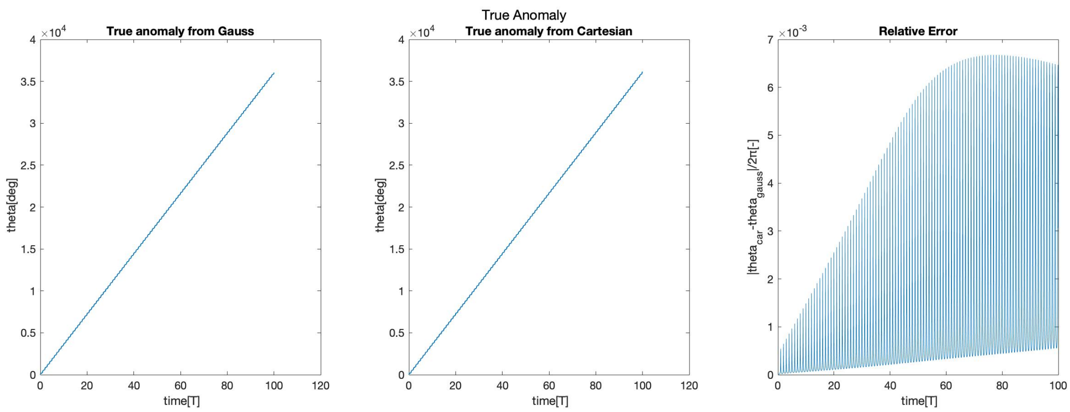

Figure 2.12: True anomaly evolution

2.7 Filtering

In the evolutions of the Keplerian Elements short and long term variations are present. Using semi-analytical methods, it could be possible to obtain for a period the long,short and secular evolution of a Keplerian element. In this case, a low-pass filter implemented in MATLAB called *movmean* was used to retrieve long-period and secular evolutions from the Keplerian elements. These figures show a comparison with the filtered evolution and the unfiltered one.

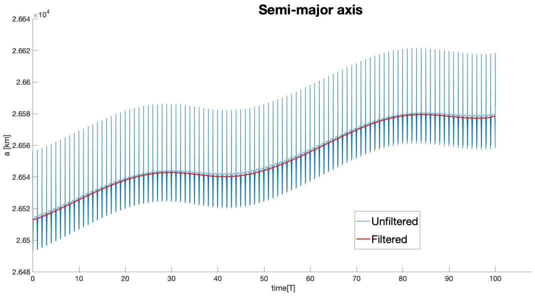

(a) semi-major axis

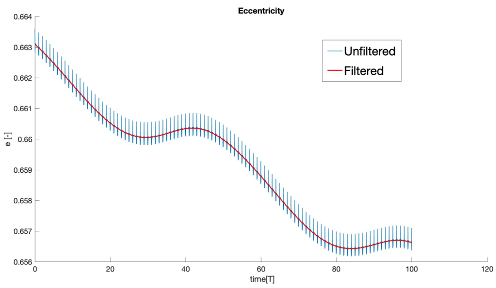

(b) eccentricity

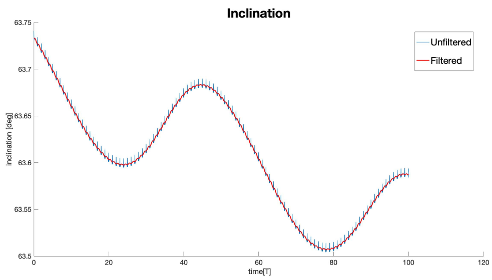

(c) inclination

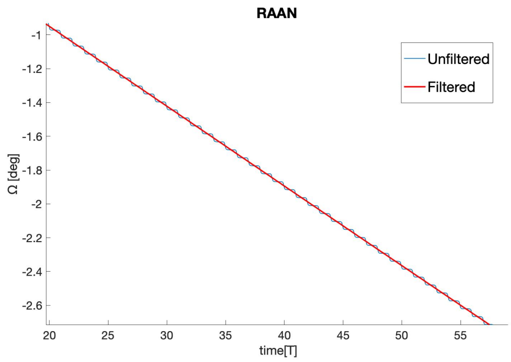

(d) RAAN

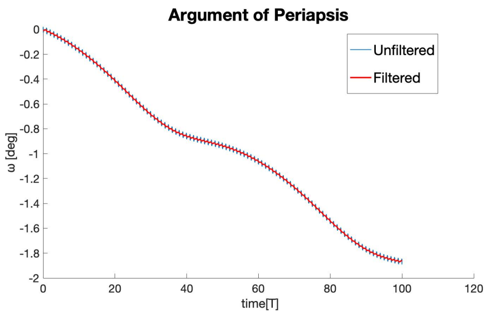

(e) Argument of periapsis

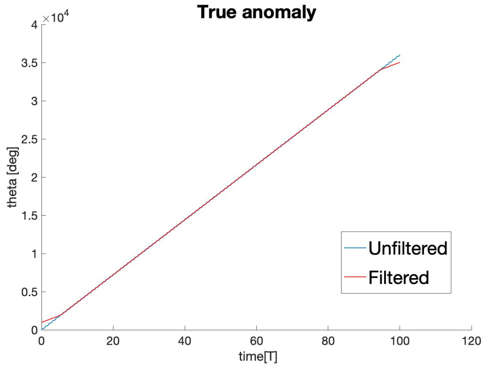

(f) True anomaly

Figure 2.13: Filtered and unfiltered Keplerian elements

2.8 Comparison with real data

In order to check the validity of the model, a satellite in the same orbital region of Space is selected using Celestrak.org, 2021, exploiting some of the properties of our orbit as filter in the search. In this way it is possible to compare the results with good approximation, since in that orbital region the real satellite's orbit is affected primarily by perturbations of Moon and Earth's oblateness (J2), even if other perturbations could be considered. The artificial satellite found is a rocket body launched in 1999 and its Keplerian elements are downloaded from NASA Horizon System for a time window of two years. The propagation of the model uses as initial conditions the same of the ones get from NASA Horizon System JPL, 2021. In the following figures the Keplerian elements obtained with the model through Gauss Equations and Cartesian coordinates are compared. True anomaly is not showed, because the real data are referred to different position of the body in its orbit, so it is not an evolution of the true anomaly.

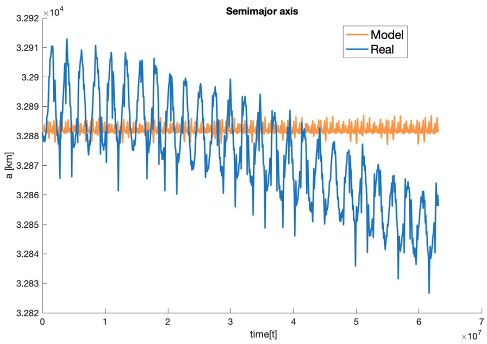

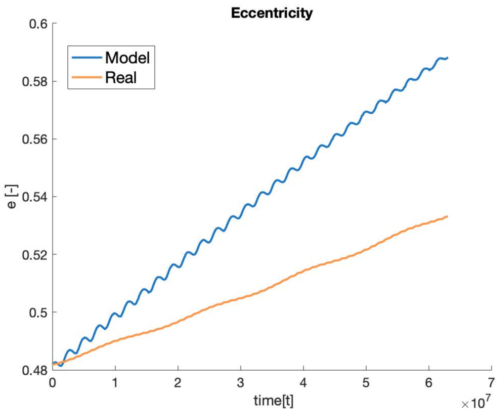

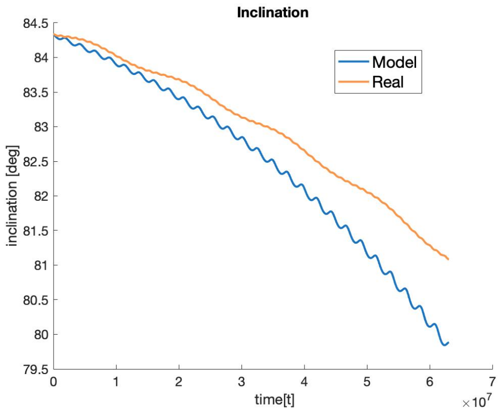

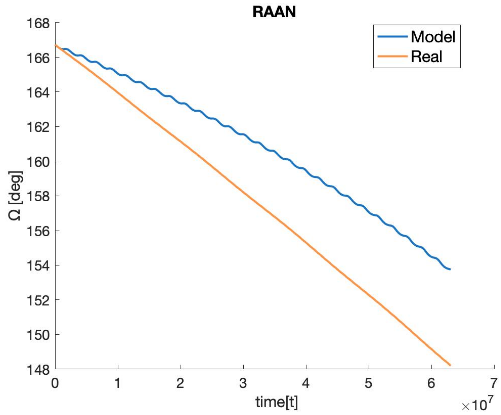

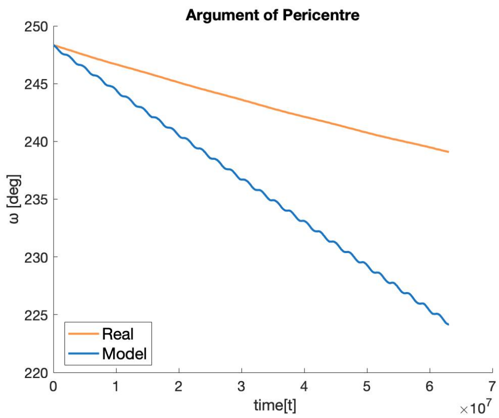

Bibliography

Celestrak.org (2021). *Satellite tracking online*. URL: https://celestrak.com/ (visited on 12/26/2021).

Curtis, Howard D. (2004). *Orbital Mechanics for Engineering Students*. Butterworth-Heinemann.

JPL (2021). *Nasa Horizon System*. URL: https://ssd.jpl.nasa.gov/horizons/app.html (visited on 12/27/2021).

NASA (2021). *Mars Atmossphere Model*. URL: https://www.grc.nasa.gov/www/k-12/airplane/atmosmrm.html (visited on 12/21/2021).